Phase-shift parametrization and extraction of asymptotic normalization constants from elastic-scattering data

O. L. Ramírez Suárez* and J.-M. Sparenberg
Physique Nucléaire et Physique Quantique, C.P. 229, Université libre de Bruxelles (ULB), B 1050 Brussels, Belgium
(Received 16 March 2016; revised manuscript received 1 July 2017; published 1 September 2017)

We introduce a simplified effective-range function for charged nuclei, related to the modified K matrix but differing from it in several respects. Negative-energy zeros of this function correspond to bound states. Positive-energy zeros correspond to resonances and "echo poles" appearing in elastic-scattering phase-shifts, while its poles correspond to multiple-of-π phase shifts. Padé expansions of this function allow one to parametrize phase shifts on large energy ranges and to calculate resonance and bound-state properties in a very simple way, independently of any potential model. The method is first tested on a d-wave $^{12}\mathrm{C}+\alpha$ potential model. It is shown to lead to a correct estimate of the subthreshold-bound-state asymptotic normalization constant (ANC) starting from the elastic-scattering phase shifts only. Next, the $^{12}\mathrm{C}+\alpha$ experimental p-wave and d-wave phase shifts are analyzed. For the d wave, the relatively large error bars on the phase shifts do not allow one to improve the ANC estimate with respect to existing methods. For the p wave, a value agreeing with the $^{12}\mathrm{C}(^{6}\mathrm{Li},d)^{16}\mathrm{O}$ transfer-reaction measurement and with the recent remeasurement of the $^{16}\mathrm{N}$ β-delayed α decay is obtained, with improved accuracy. However, the method displays two difficulties: the results are sensitive to the Padé-expansion order and the simplest fits correspond to an imaginary ANC, i.e., to a negative-energy "echo pole," the physical meaning of which is still debatable.

DOI: 10.1103/PhysRevC.96.034601

I. INTRODUCTION

Low-energy nuclear reactions, in particular those relevant to nuclear astrophysics [1], are a fascinating application field for quantum scattering theory [2]. Because of the Coulomb repulsion between nuclei, cross sections are often impossible to measure directly and theoretical extrapolations are indispensable. The simplest of these reactions, elastic scattering, is theoretically described with a partial-wave decomposition, each partial wave l being fully characterized by a nuclear phase shift δ_l or scattering matrix $S_l = e^{2i\delta_l}$, both functions of the energy. Resonances appear as fast increases of δ_l at real positive energies or as poles of S_l at complex energies. For some reactions subthreshold bound states at small negative energies also play an essential role. This is for instance the case for the 1^- and 2^+ bound states lying just below the $^{12}\mathrm{C}+\alpha$ threshold which strongly affect the $^{12}\mathrm{C}(\alpha,\gamma)^{16}\mathrm{O}$ cross section, an important reaction for stellar evolution [3]. For these states, energies are usually well known experimentally, but their wave-function asymptotic normalization constant (ANC) is not. These are generally deduced from indirect experimental data, like β-delayed α emission [4,5] or α-transfer reactions [6].

A natural way to extract an ANC for a given l is to parametrize the experimental δ_l and to extrapolate at negative energies, as bound states also correspond to S_l poles [2]. A usual tool to do so is the reaction (R) matrix [7,8], which describes both resonant and bound states as poles characterized by real energies and reduced width amplitudes (Mittag-Leffler expansion). This motivated the high-precision measurement of $^{12}\mathrm{C}+\alpha$ scattering [9,10] but led to a very loose constraint on the 1^- ANC [9] and to a questionable constraint on the 2^+ ANC [11]. The background δ_l (between resonances) are indeed described in terms of a channel radius and of a high-energy large-width pole, which adds several parameters with no direct physical meaning to the fit. Hence, simpler parametrizations are necessary.

A first option is the effective-range function (ERF) K_l of Eq. (2) [12]. Its analyticity properties imply the existence of a Maclaurin expansion, the effective-range expansion [2], which provides both a parametrization of δ_l and an access to subthreshold-bound-state ANCs [13,14]. This expansion is generally limited to low energies, which restricts the analysis of experimental data [15], but this could be overcome by the use of Padé approximants [13,16–18]. A more serious drawback is that K_l is a weakly sensitive quantity: very close ERFs can lead to very different, sometimes unphysical, δ_l and ANCs [15,19]. This flaw is due to the second (h) term of Eq. (2); it can be avoided by directly expanding the first term of Eq. (2), which is actually related to the inverse of the modified K matrix $\mathcal{K}_l$ [20–22] (see below). Strangely enough, we could not find an explicit connection between K_l and $\mathcal{K}_l$ in the literature. Like the R matrix, $\mathcal{K}_l$ is usually Mittag-Leffler expanded. The background description does not require a channel radius but is however complicated, in particular through the use of complex pole energies and reduced width amplitudes [23,24]. For $^{12}\mathrm{C}+\alpha$ both methods lead to similar ANC constraints [4].

Here, we instead propose to expand function Δ_l of Eq. (3), which can be considered a simplified K_l or $\mathcal{K}_l^{-1}$. Function Δ_l also appears in quantum-defect theory for attractive Coulomb potentials [25] and has the same expression for all l's (no w_l function). This is desirable because the Coulomb potential

*Present address: Grupo de Simulación, Análisis y Modelado (SiAMo) Universidad ECCI, Bogotá, Colombia.

dominates the centrifugal potential at large distances; hence, the low-energy phase-shift behavior should only depend on the Coulomb potential, not on l. We also show that a Padé approximant is more efficient than a Mittag-Leffler expansion, with fewer, more physical, but possibly complex parameters, hence leading to better constraints on the $^{12}\mathrm{C}+\alpha$ ANCs from δ_l parametrizations.

II. SIMPLIFIED EFFECTIVE-RANGE FUNCTION

We consider the elastic scattering of two particles of charges Z_1e and Z_2e at positive center-of-mass energy $E=\frac{\hbar^2}{2\mu}k^2$, with k the wave number and μ the reduced mass. The scattering matrix reads [1,2]

$$S_l^{\mathrm{tot}}=e^{2i\sigma_l}e^{2i\delta_l}\equiv\frac{\Gamma(l+1+i\eta)}{\Gamma(l+1-i\eta)}\times\frac{\cot\delta_l+i}{\cot\delta_l-i}, \tag{1}$$

while the usual effective-range function reads [12,13]

$$K_l=\frac{2w_l}{l!^2a_N^{2l+1}}\left[\frac{\pi\cot\delta_l}{e^{2\pi\eta}-1}+\mathrm{Re}\,h\right], \tag{2}$$

with the Coulomb phase shifts σ_l, $\eta=1/a_Nk$ and the nuclear Bohr radius $a_N=4\pi\epsilon_0\hbar^2/\mu Z_1Z_2e^2$. The complicated functions $w_l=\prod_{j=0}^{l}[1+(j/\eta)^2]$ and $h=\psi(i\eta)-\ln(i\eta)+\frac{1}{2i\eta}$, where ψ is the digamma function, are aimed at improving the analyticity properties of K_l^c, the analytic continuation of K_l in the complex plane [12].

Here we use the simpler function (see also [26–29])

$$\Delta_l=\frac{2\pi}{a_N}\frac{\cot\delta_l}{e^{2\pi\eta}-1}, \tag{3}$$

which does not require the use of functions w_l and h. In the limit $\eta\to0$, it reduces to the standard $l=0$ ERF for the neutral case, $k\cot\delta_0$. Equations (1) and (3) lead to the expression of the nuclear scattering matrix in terms of Δ_l,

$$S_l=\frac{a_N(e^{2\pi\eta}-1)\Delta_l+i\,2\pi}{a_N(e^{2\pi\eta}-1)\Delta_l-i\,2\pi}, \tag{4}$$

while Eqs. (2) and (3) directly relate K_l to Δ_l as

$$K_l=\frac{w_l}{l!^2a_N^{2l}}\left[\Delta_l+\frac{2\,\mathrm{Re}\,h}{a_N}\right], \tag{5}$$

where the first term is nothing else than the inverse of the modified K matrix [20–22],

$$\mathcal{K}_l=\frac{l!^2a_N^{2l}}{w_l\Delta_l}. \tag{6}$$

This last relation can be derived from Eqs. (2.2), (2.3), and (3.4) of Ref. [30]. It implies that the zeros and poles of Δ_l and $\mathcal{K}_l$ are exchanged. We will see below that it also implies that $\mathcal{K}_l$ can be more energy dependent than Δ_l for $l>0$, which makes it less easy to parametrize.

Let us now study the properties of Δ_l for real energies. For $E>0$, Eqs. (3) and (4) imply that Δ_l is real, keeps S_l unitary, has N_0 zeros $E=E_{0,j}$, $j=1,\ldots,N_0$ and N_∞ poles $E_{\infty,j}$, $j=1,\ldots,N_\infty$ satisfying

$$\frac{\delta_l(E)}{\pi/2}=\begin{cases}\text{even} & \text{for } E=E_{\infty,j} \quad (j=1,\ldots,N_\infty),\\ \text{odd} & \text{for } E=E_{0,j} \quad (j=1,\ldots,N_0).\end{cases} \tag{7}$$

These characterize the general structure of the phase shift for positive energies. Neglecting the energy variation of the denominator in the vicinity of energies $E_{0,j}$, Eq. (3) implies that the derivative of the phase shift at these energies is simply related to the slope of Δ_l through

$$\left.\frac{d\delta_l}{dE}\right|_{E=E_{0,j}}\approx-\frac{a_N}{2\pi}(e^{2\pi\eta_{0,j}}-1)\left.\frac{d\Delta_l}{dE}\right|_{E=E_{0,j}}. \tag{8}$$

This allows us to distinguish *resonances*, which correspond to an increasing phase shift and a decreasing Δ_l function, from "*echo poles*", which correspond to a decreasing phase shift and an increasing Δ_l function [21]. For narrow resonances, the phase-shift variation can be very quick; in a single-zero approximation, the resonance energy is simply $E_{0,j}$ and its width Γ_j reads

$$\Gamma_j\approx\frac{4\pi}{a_N(e^{2\pi\eta_{0,j}}-1)}\left[-\frac{d\Delta_l}{dE}\right]^{-1}_{E=E_{0,j}}. \tag{9}$$

For "echo poles", in contrast, the phase-shift variation is slow, with large negative "widths"; these characterize the background structure of the phase shift and are not to be considered resonances. The first factor of Eq. (9) is rapidly varying with energy and is to be considered a purely Coulomb penetration factor. The derivative of Δ_l is then a reduced width, the square root of which is a reduced-width amplitude. Resonances thus correspond to real reduced-width amplitudes, while "echo poles" correspond to imaginary ones.

For $E=0$, if the scattering length $a_l=-1/K_l(0)$ does not vanish, Δ_l admits a Maclaurin expansion because K_l, w_l, and h admit one. Since $w_l(0)=1$ and $h(0)=0$, one gets $\Delta_l(0)=-l!^2a_N^{2l}/a_l$ and the phase-shift behavior $\delta_l\propto e^{-2\pi\eta}$ for $E\to0^+$. For $E\to\infty$, one has $\delta_l\propto k^{-1}$ and hence $\Delta_l\propto E$, assuming the nuclear potential is regular enough and neglecting relativistic effects [2].

For $E<0$, K_l^c has to be used. It is real and satisfies

$$K_l^c(E_B)=\left.\frac{2w_l}{l!^2a_N^{2l+1}}h\right|_{\eta=\eta_B}, \tag{10}$$

for the bound-state energy $E_B=\frac{\hbar^2}{2\mu}k_B^2$ and the imaginary parameter $\eta_B=1/(a_Nk_B)$ [13,31]. This means that Δ_l^c, the analytic continuation of Δ_l, vanishes at $k=k_B$,

$$\Delta_l^c(E_B)=0, \tag{11}$$

a much simpler condition than the corresponding one for the usual ERF (10). As expected, this zero of Δ_l^c corresponds to a pole of the modified K matrix (6); the properties of the K-matrix poles then imply that these zeros of Δ_l^c are simple. Moreover, similarly to resonance widths, bound-state ANCs have a simple expression in terms of Δ_l^c: the usual ERF formula of Ref. [13] reads

$$\mathrm{ANC}=\frac{\Gamma(l+1+|\eta_B|)}{|\eta_B|^l}\left[-w_l(\eta_B)\frac{d\Delta_l^c}{dk^2}\right]^{-1/2}_{k=k_B}, \tag{12}$$

which, again, does not depend on h. Let us stress at this point that Δ_l^c has to be a decreasing function of the energy for the ANC to be a real quantity, showing the continuity between positive-energy resonances and negative-energy bound states. However, in the following, we will discuss the possible interest of *negative-energy* "echo poles", corresponding to increasing Δ_l^c, i.e., to *imaginary ANCs*.

Altogether, we thus expect Δ_l^c to be well approximated in the whole complex-E plane by the Padé approximant

$$\Delta_l^c \approx \frac{\sum_{i=0}^{N} p_i E^i}{\sum_{i=0}^{M} q_i E^i} \times \frac{\prod_{n=1}^{N_B}\left(1-\frac{E}{E_{B,n}}\right)\prod_{j=1}^{N_0}\left(1-\frac{E}{E_{0,j}}\right)}{\prod_{j=1}^{N_\infty}\left(1-\frac{E}{E_{\infty,j}}\right)}, \quad (13)$$

with p_i and q_i real parameters, $N \geqslant 0$, and

$$M = N + N_0 - N_\infty - 1 + N_B \geqslant 0. \quad (14)$$

Note that without loss of generality we can choose $p_0 = 1$, which implies $q_0 \approx -a_l/l!^2 a_N^{2l}$.

We can corroborate hypothesis (13) by fitting the sets $\{p_i\}$ and $\{q_i\}$ to collectively describe the details of the experimental phase shifts, via Eq. (3) and with values of N and M as small as possible. Resonance energies E_r and widths Γ can then be computed by finding the complex poles $E_{\rm pole} = E_r - \frac{i}{2}\Gamma$ of the scattering matrix (4), which is a more general method than the one based on phase shifts only.

Regarding bound-state ANCs, they can be computed analytically by combining Eqs. (12) and (13). For a weakly bound state, we expect the following linear approximation to be precise between $E = 0$ and E_B:

$$\Delta_l(E) \underset{E\in[E_B,0]}{\approx} \frac{l!^2 a_N^{2l}}{-a_l}\left(1-\frac{E}{E_B}\right). \quad (15)$$

From there and Eq. (12), we deduce an approximate expression for the ANC in terms of the scattering length,

$$\text{ANC} \approx \frac{\Gamma(l+1+|\eta_B|)}{l!}|k_B|^{l+1}\sqrt{\frac{a_l}{w_l(\eta_B)}}. \quad (16)$$

These equations show that the presence of a standard subthreshold bound state corresponds to a (possibly large) positive scattering length. A subthreshold "echo pole", on the other hand, would correspond to a negative scattering length.

III. FITS OF ^{12}C + α PHASE SHIFTS

As a first application, we consider the important $^{12}C + \alpha$ system, for which $\hbar^2/2\mu \approx 6.9635$ MeV fm^2 and $a_N \approx 0.80598$ fm. A convenient feature of this system, in addition to the quality of the available experimental data, is the existence of simple potential models allowing a theoretical check of our method.

A. *d*-wave potential model

To test the method, we first apply it to the $^{12}C + \alpha$ d-wave potential of Refs. [11,14], which has three bound states ($N_B = 3$) and no narrow resonance. The most weakly bound state occurs at the experimental energy $E_B = -244.85$ keV below the $^{12}C + \alpha$ threshold, with an ANC of 138.4×10^5 fm$^{-1/2}$. It is expected to qualitatively describe the cluster structure of this subthreshold state. The absence of narrow resonances, on the other hand, physically corresponds to the absence of low-energy 2^+ states with a marked $^{12}C + \alpha$ structure in the ^{16}O spectrum. The two other bound states occur at much lower energies and are physically forbidden, simulating the Pauli exclusion principle between nucleons of the ^{12}C and α nuclei. All three bound states have to be taken into account in the Levinson theorem, which implies that the phase shift continuously decreases from 3π at zero energy down to 0 at infinite energy. Consequently, it crosses twice an integer multiple of π and thrice a half-integer multiple of π on the whole positive-energy semi-axis, hence $N_0 = 3$ and $N_\infty = 2$ for this potential. Let us stress that the corresponding three zeros of the Δ_2 function are associated with positive slopes for Δ_2 and negative slopes for the phase shift, hence with negative "widths" and with imaginary reduced-width amplitudes [see Eq. (9)]. These are "echo poles" describing the phase-shift background behavior.

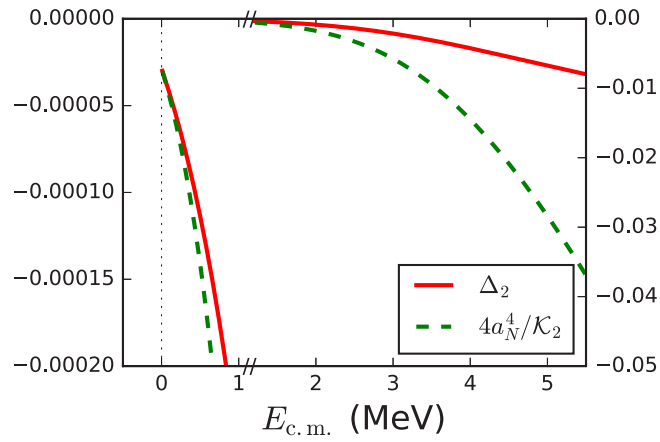

FIG. 1. Simplified effective-range function Δ_2 (red solid line) and renormalized inverse of the modified K matrix (green dashed line) deduced from the elastic-scattering phase shift of the d-wave $^{12}C + \alpha$ potential model of Refs. [11,14]. The y-axis scale changes at 1.1 MeV.

On this potential model, we first checked that a Padé approximant of the Δ_2 function is a very efficient way of parametrizing phase shifts over large energy ranges [32]. For instance, with $N = 1, M = 4$ in Eq. (13), one can fit the phase shifts up to 2.4 GeV. This confirms that, with Padé approximants, effective-range expansions are not restricted to low energies anymore.

On the other hand, we also checked that the low-energy behavior of Δ_2 can be used to deduce the subthreshold-bound-state ANC from scattering phase shifts. This is illustrated in Fig. 1, where Δ_2 is shown to have an approximately linear behavior at very low energies (i.e., below 300 keV). Extrapolating this linear behavior at negative energies leads to a rather precise bound-state-energy estimate: Δ_2 crosses the energy axis at -213 keV, which only differs by 13% from the correct binding energy. A second-order extrapolation

provides −229 keV (7% error). This confirms the validity of our hypothesis that Δ_2 can be continued from positive to negative energies, linking low-energy phase shifts with properties of the subthreshold bound state. The slope of this Δ_2 linear extrapolation being negative, Eq. (16) can be used to evaluate the corresponding ANC. With $a_2 = 58\,910$ fm^5 for this potential, this provides an ANC $\approx 130.5 \times 10^5$ fm$^{-1/2}$, i.e., a 6% error. This is to be compared with the 11% error obtained from Eq. (19) of Ref. [14], which is based on a linear approximation of $\Delta_2 w_2$. Indeed, Fig. 1 also shows that Δ_2 has a weaker energy dependence than $\Delta_2 w_2 = 4a_N^4/\mathcal{K}_2$ (both functions having the same value at zero energy), which explains its more efficient analytical approximation. Finally, a second-order extrapolation for Δ_2 reproducing both the scattering length and the effective range $r_2 = 0.1580$ fm^{-3} for this potential leads to an ANC $\approx 137.0 \times 10^5$ fm$^{-1/2}$, i.e., a 1% error.

In conclusion, this potential-model study shows that the analytic continuation of the simplified effective-range function Δ_l is probably the best possible option to deduce bound-state properties from elastic-scattering phase shifts. In particular, it is much simpler and more efficient than the standard effective-range function (see also below). It is related to the inverse of the modified K matrix but is even simpler and more precise. However, as illustrated by Fig. 1, the accuracy of the extracted bound-state properties are expected to strongly depend on the energy domain on which Δ_l varies smoothly. Equation (16) in particular assumes a linear dependence for the simplified effective-range function, which might be valid on a small energy interval only. Moreover, this equation can only be used when the scattering length is known, which is the case for a theoretical model only. Some difficulties are thus expected if the method is used to analyze experimental data: First, larger energy intervals might be required if experimental data are not available at low energies. Consequently, a linear approximation will not be sufficient and a larger number of parameters will be required. Second, among these parameters, the scattering length will have to be extracted from data too. Binding energies, in contrast, will be available from experiment and will not have to be deduced from phase shifts. With this tool in hand and these restrictions in mind, let us now switch to the analysis of experimental data for the $^{12}\mathrm{C} + \alpha$ system.

B. *p*-wave experimental data

We apply our method to the phase shifts of Refs. [9,10], which have been obtained through an R-matrix fit of high-precision cross sections measured on the energy interval [1.955, 4.965] MeV. For the 1^- phase shifts [see Fig. 2(a)], the resonance at 2.4 MeV is clearly seen and a threshold effect or the tail of a higher-energy resonance can be guessed above 4.1 MeV. To simplify the following discussion and since we are interested in low-energy extrapolation towards the subthreshold bound-state energy at $E_B = -0.045$ MeV, we do not take data above 4.1 MeV into account (we have checked that our conclusions are essentially unaffected by keeping them). The corresponding Δ_1 function behaves like $-6.6929 \times 10^{-5}(E - E_{\mathrm{res}})$ fm^{-1} for $E \approx E_{\mathrm{res}} = 2.442$ MeV. As expected, it displays a zero at the resonance energy and a negative slope, which leads to the width estimate $\Gamma \approx 360$ keV using Eq. (9). By dividing Δ_1 by $1 - E/E_{\mathrm{res}}$, one gets the "no res." data of Fig. 2(b), which are approximately linear below 4.5 MeV.

Remarkably, extrapolating these data towards negative energy leads to a zero close to E_B, as shown by our [2/0] fit (detailed below). This suggests that Δ_1 relates the subthreshold bound state to the experimental phase shifts in a very simple way, despite a 2-MeV gap between the lowest elastic-scattering measurement and the bound state. This is not the case for $\mathcal{K}_1^{-1}$, also represented in Fig. 2(b): it depends more strongly on the energy, and a linear fit does not provide the correct binding energy. The K-matrix Mittag-Leffler fit of Ref. [4] (adjusted using older data) is also represented in Figs. 2(a) and 2(b); although the phase shifts are satisfactory, $1/\mathcal{K}_1$ presents a complicated structure, due to the background description and to an imposed real reduced-width amplitude for the bound state, which leads to a negative slope of $1/\mathcal{K}_1$ at the bound-state energy and to a pole of $1/\mathcal{K}_1$ (and a zero of δ_1) at low positive energy. A similar picture is obtained for the more recent R-matrix fit of Refs. [9,10], which also corresponds to a real reduced-width amplitude for the bound state.

In contrast, our Padé fit is much simpler but it corresponds to a small but positive slope of Δ_1 at the bound-state energy, and hence to an imaginary reduced-width amplitude and an imaginary ANC, according to Eq. (12). This seems to disagree with usual properties of "echo poles", which generally occur at high energies, and with general results from the R-matrix theory [23], where only real reduced-width amplitudes are used. In Ref. [21], a general theoretical discussion of the sign of these widths is made, where they are indeed shown to be generally positive for low-energy states. However, a negative sign is also proved to be possible (see Eq. (8.4) and Sec. IX of Ref. [21]) when the state has a structure dominated by other channels, in particular neutral ones. The present state indeed has a structure dominated by a single-particle mean-field configuration rather than by a $^{12}\mathrm{C} + \alpha$ cluster structure. This is the reason why it does not show up in a simple $^{12}\mathrm{C} + \alpha$ potential model, contrary to the d-wave subthreshold state. However, the closest neutral channel being the $^{15}\mathrm{O} + n$ channel, with a threshold energy lying 8.5 MeV above the $^{12}\mathrm{C} + \alpha$ one, it is unclear whether it is sufficient to justify the use of a low-energy "echo pole". This hypothesis should be tested, e.g., in an R-matrix model coupling charged and neutral channels, a project we defer to a future work. In the meanwhile, we choose here to further explore the fits obtained with a single-channel imaginary ANC, as the simplicity of the corresponding Δ_1 function is quite appealing. Moreover, we will see below that, except for its phase, the deduced ANC agrees with totally independent measurements, a fact which seems hard to consider as a simple coincidence.

Also represented in Figs. 2(a) and 2(b) are the δ_1 and nonresonant Δ_1 corresponding to the three-term effective-range expansion of Ref. [19]; they are clearly unsatisfactory. Interestingly, all these fits correspond to practically indistinguishable K_1, as shown in Fig. 2(c), where all curves superimpose. This illustrates the lack of sensitivity of the usual effective-range function to low-energy physical quantities, due

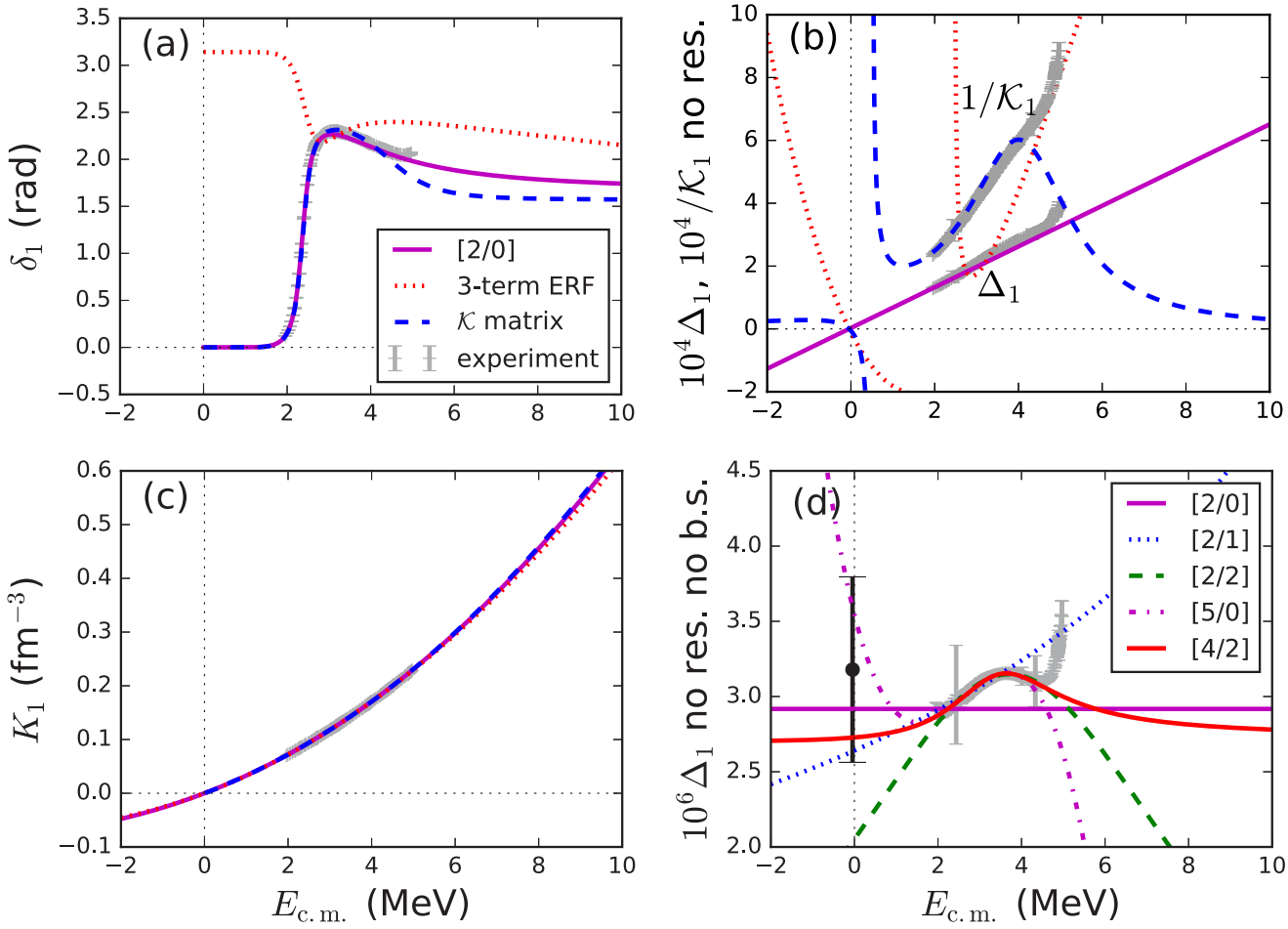

FIG. 2. $^{12}\mathrm{C}+\alpha$ elastic-scattering p-wave (a) phase shifts δ_1, (b) simplified effective-range function (ERF) with resonance zero removed, $\Delta_1/(1-E/E_{\rm res})$, (c) usual ERF K_1, (d) simplified ERF with resonance and bound-state zeros removed, $\Delta_1/(1-E/E_{\rm res})(1-E/E_B)$, compared with the value (black point with error bar) deduced from the transfer-reaction ANC of Ref. [6] (after a sign change; see text). The experimental data (gray crosses) are from Ref. [9,10] and the $[N_{\rm fit}/M_{\rm fit}]$ Padé approximants are detailed in the text. In (a), (b), and (c), the standard ERF fit of Ref. [19] and the modified K-matrix fit of Ref. [4] are also shown. In (c), the three theoretical curves are indistinguishable from the experimental data.

to the second (h) term in Eq. (2), which strongly dominates the first term here.

Since the slope of Δ_1 at the bound-state energy directly provides the ANC (12) and since the bound-state energy is precisely known experimentally, we again divide Δ_1 by $1-E/E_B$, which leads to the "no res. no b.s." data of Fig. 2(d). This reveals even more details. Ideally, the resulting curve should be a constant directly providing the ANC. However, the situation is not that simple. Except for a rather fast variation above 4.1 MeV (much more clearly seen on Δ_1 than on δ_1), the background Δ_1 function is only *approximately* constant: it varies between 2.8 and 3.7×10^{-6}, which corresponds to an ANC of $i\,214(6)\times10^{12}$ fm$^{-1/2}$. Except for the phase factor, this is in perfect agreement and already thrice more accurate than the value of Ref. [6], $208(20)\times10^{12}$ fm$^{-1/2}$, which corresponds to the black dot of Fig. 2(d). Since the error bars on the phase shifts are very small, a better accuracy on the ANC might even be in reach, but this requires fitting the bell-shaped structure that appears on the experimental background Δ_1 function, with a maximum reached at 3.7 MeV. In the following, we assume this structure is physical. However, it would probably be wise to revisit experimental data, e.g., using Eq. (13) for a multienergy phase-shift analysis, to confirm that this structure is not due to an underestimate of the phase-shift error bars.

Figure 2(d) presents several fits of the data, obtained by a two-step procedure. First we solve a linear-algebra system providing the coefficients of an $[N_{\rm fit},M_{\rm fit}]$ Padé expansion of Δ_1 (the resonance and bound-state energies are allowed to slightly vary), without taking error bars into account. The total number of free parameters is $N_{\rm fit}+M_{\rm fit}+1$; they can be formulated as $N_{\rm fit}=N_0+N_B+N$ zeros, $M_{\rm fit}=N_\infty+M$ poles (possibly complex), and the scattering length a_l. Condition (14) is relaxed, as we fit data on a small energy interval. Second, we start from the obtained parameters to perform a least-squares minimization, applied on the randomized data of Refs. [9,10]. An estimate of the ANC error bar $\sigma_{\rm ANC}$ can then be obtained from Eq. (16), and it reads

$$\frac{\sigma_{\rm ANC}}{|{\rm ANC}|}\approx\frac{1}{2}\frac{\sigma_{a_l}}{|a_l|}, \tag{17}$$

where σ_{a_l} is the uncertainty on the scattering length. As expected from the size of the error bars in Fig. 2(d), each of these fits provides a very accurate ANC, which shows the power of our method. For instance, a [2/0] fit (solid magenta curves in Fig. 2) on the reduced energy interval [1.955, 2.48] MeV (to get a χ^2 per point smaller than 1) leads to an ANC $= i\,215(1) \times 10^{12}$ fm$^{-1/2}$, which corresponds to the low-energy plateau of the background Δ_1 function. However, a [2/1] fit on [1.955, 3.88] MeV, which has a stronger slope, leads to the incompatible value $i\,226(1) \times 10^{12}$ fm$^{-1/2}$. The [2/2], [5/0], and [4/2] fits on [1.995, 4.1] MeV bring $i\,258(2)$, $i\,194(8)$, $i\,223(4) \times 10^{12}$ fm$^{-1/2}$ respectively. Most fits with other orders lead to unphysical or merging poles and zeros.

This illustrates a difficulty of our method: since it requires an extrapolation on a rather large energy interval, different orders can lead to incompatible ANC values. In the present case, we choose to combine the ANC estimates of the [2/0], [2/1], and [4/2] fits to get what we consider to be the most plausible estimate,

$$C_1 = i\,220.5(6.5) \times 10^{12}\text{fm}^{-1/2}. \tag{18}$$

This excludes the [2/2] fit, which is accurate but incompatible with the transfer-reaction data, and the less accurate [5/0] fit. Let us also stress that these two fits display a very strong decrease above 4.1 MeV, which does not follow the trend of the experimental data. The [4/2] fit, in contrast, is probably the most satisfactory, as it displays a plateau at low and at high energies, in agreement with the trend shown by experimental data. It is also close to the very simple [2/0] fit but with a much better χ^2; in particular, on the scale of Figs. 2(a)–2(c), curves based on this [4/2] fit would be practically indistinguishable from the [2/0] ones, hence the solid lines used for both in Fig. 2(d).

Estimate (18) should thus be taken with caution, as both the imaginary phase and the error estimate are still subject to discussions. However, let us stress that, for the 1^- subthreshold state, (i) the R-matrix fit itself did not bring any useful information on the ANC [10]; (ii) in particular, this fit was compatible with a vanishing reduced-width amplitude for the subthreshold state, which could be related to the imaginary amplitude obtained here; (iii) our fits favor a slightly larger value of the ANC than that of Ref. [6], which in turn is marginally compatible but also larger than the values deduced from the β decay of ^{16}N [4]. However, a new measurement of the relevant $\beta\alpha$ branching ratio [5] suggests that the estimates of Ref. [4] were indeed underestimated; with the new branching ratio value, the β decay data agree very well with the transfer-reaction ones, and hence with our new estimate from scattering phase shifts.

In conclusion, we consider this first application of our method to experimental data to be promising; some discussions are still open but they suggest interesting future research, both experimentally [confirming the structure revealed by Fig. 2(d)] and theoretically (confirming the imaginary phase of the ANC). Let us finally remark that a Padé approximant of the Δ_1 function allows a direct computation of the complex-plane S_1 pole using Eq. (4). All the above approximants lead to a resonance energy 2.3657(4) MeV and width 351(2) keV,

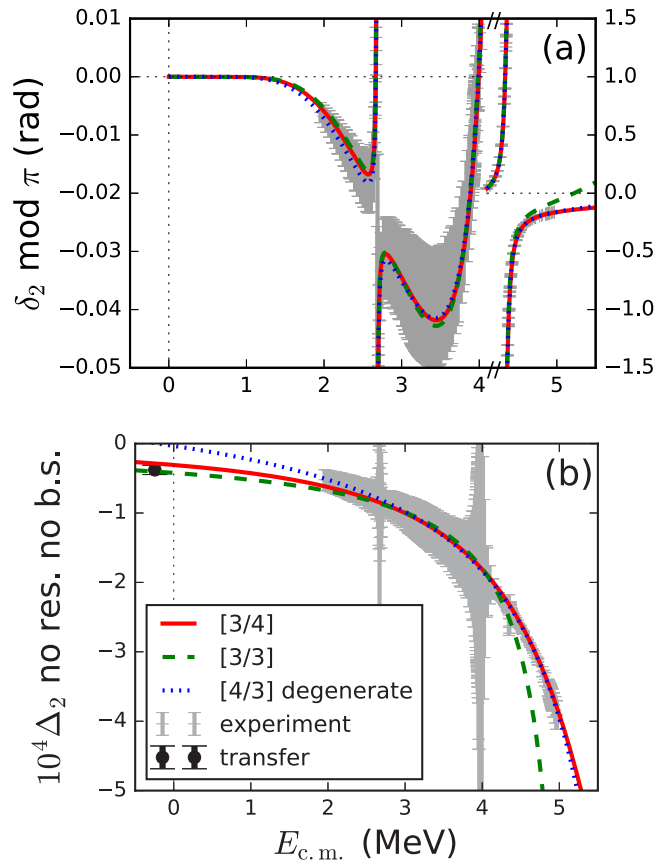

FIG. 3. Same as Fig. 2(a) and 2(d) for the d wave, with two resonances ($N_0 = N_\infty = 2$) and one subthreshold bound state ($N_B = 1$) removed. The y axis changes at 4.1 MeV in (a).

in excellent agreement with the similar method developed in Ref. [33] and with the rough estimates given above, based on a linear approximation of Δ_1.

C. d-wave experimental data

Let us now turn back to the 2^+ wave, for which we follow the same steps as those just followed for the p wave. For the d wave, there is a bound state at $E_B = -244.85$ keV, as discussed above. In addition, from the experimental phase shifts δ_2 we find $E_{0,j} = \{2.683, 4.357\}$ MeV and $E_{\infty,j} = \{2.667, 3.981\}$ MeV, which correspond to the two well-known resonances visible on the experimental phase shifts δ_2 [Fig. 3(a)]. Let us stress that these two resonances do not have a $^{12}\text{C} + \alpha$ structure, which is why they did not appear in the simple potential model of Sec. III A. Building the corresponding Δ_2 function and removing these three zeros and two poles leads to the function plotted in Fig. 3(b). Comparing this figure with the corresponding one for the p wave [Fig. 2(d)] shows that the situation is much less favorable here, except for the sign which is now negative, as expected from Eq. (12). First, the background Δ_2 function is strongly energy dependent on the experimental energy range. Actually, the best fits obtained for this function favor an additional zero around the threshold energy, which would correspond to an additional bound or resonant 2^+ state in this region. This

is illustrated for instance by the [4/3] fit of Fig. 3, which displays an excellent χ^2 per point of 0.49 on the whole energy range, with only three parameters for the background: one zero close to (or degenerate with) the subthreshold bound state, one pole at about 6.3 MeV, and the scattering length. Although the existence of a degenerate subthreshold state is unlikely, testing this hypothesis might be interesting, both from the experimental and theoretical points of view.

Second, despite their good accuracy, the phase shifts of Ref. [10] lead to rather large error bars on the background Δ_2 function [gray area of Fig. 3(b)]. Hence, the extrapolation of this function towards low energies is inaccurate and the prediction for the ANC is not expected to improve on the one of Ref. [6], ANC $= 114(10) \times 10^3$ fm$^{-1/2}$ [black dot of Fig. 3(b)]. Indeed, rather different values for the ANC can be obtained with different fit orders. For instance, the [3/3] and [3/4] fits of Fig. 3, which present no degenerate bound state because $N = 0$, lead to ANCs of $110(11) \times 10^3$ fm$^{-1/2}$ and $131(15) \times 10^3$ fm$^{-1/2}$ respectively. The [3/3] fit has a χ^2 per point of 0.54 but is limited to energies lower than 4.3 MeV, as it fails to reproduce high- and low-energy data together. Moreover, it reaches the upper end of the phase-shift error bars at low energies; choosing a larger energy interval brings the fit outside these error bars and hence leads to an even smaller value for the ANC. Similar results are obtained for the [4/3] fit, forcing the additional zero to stay at large positive energies [32]. The [3/4] fit, in contrast, is able to fit the data on the whole interval, again with three parameters for the background. The corresponding ANC is compatible with the values of both Refs. [10] and [11], hence making any definite conclusion hazardous. Fits with $N = 0$ and larger M lead to larger values for the ANC but with even larger error bars. Let us mention a final difficulty of our method in a case like this, with rather large error bars: by construction, we only explore one small region of the parameter space at a time. Hence, only local minima are considered and they are determined by the initial values chosen for the parameters. These initial values are deduced from the (smooth) R-matrix phase shifts. We have checked that a more sophisticated method, based on a direct calculation of the Padé-approximant coefficients from randomized data, leads to essentially the same results for the d-wave fits just presented [32].

IV. CONCLUSIONS

To sum up, our new phase-shift analysis method, based on a simplified effective-range expansion Δ_l given by Eq. (3), allows one to describe δ_l in a wide energy range and directly provides ANC estimates for subthreshold bound states. It relies on two sets of parameters: one fixed $\{E_0, E_\infty, E_B\}$ with a direct physical meaning and another free $\{p_i, q_i\}$ with a minimal number of parameters, among which is the scattering length. We have tested it on a $^{12}\mathrm{C} + \alpha$ d-wave potential model and shown that it is more efficient than methods based on the traditional effective-range function, or even on the modified K matrix. In particular, the analytic continuation of Δ_l at negative energies was shown to be very useful. This should still be fully justified from the mathematical point of view, as up to now only the traditional effective-range function is proved to have the necessary analyticity properties on the whole complex wave-number plane. We expect the proof to be related to the one developed for the modified K matrix [21].

When used for the analysis of experimental $^{12}\mathrm{C} + \alpha$ phase shifts, the method leads to better and simpler constraints on the subthreshold bound-state ANCs than the R matrix, modified K matrix, or traditional effective-range function. For the d wave, an accuracy similar to the best ones available today is obtained, but no improvement can be reached because of the still relatively large error bars and because of the complicated functional dependence of Δ_2 between the lowest-energy experimental phase shift and the subthreshold bound state. For the p wave, a structure hidden up to now is revealed from the data, which deserves further experimental study, and a simple linear behavior seems to connect the experimental data with the subthreshold bound state. However, this simple behavior is associated with an imaginary ANC or reduced-width amplitude, the meaning of which should still be clarified from the theoretical point of view, probably through coupled-channel effects. Regarding accuracy, the new p-wave ANC estimate is promising, showing a factor-3 is gain with respect to existing results, and a factor-10 improvement could be in reach. However, the order choice for the Padé approximants of Δ_1 is delicate, as different choices lead to accurate but incompatible values for the ANC.

In the future, we plan to apply our method to other systems and to extend it to coupled channels and to capture reactions.

ACKNOWLEDGMENTS

This text presents research results of the IAP program P7/12 initiated by the Belgian-state Federal Services for Scientific, Technical, and Cultural Affairs, which supported O.L.R.S. during his Ph.D. work in Brussels. We thank D. Baye, C. Brune, P. Descouvemont, R. Johnson, R. Raabe, and N. Timofeyuk for useful discussions at various stages of this work, as well as the Python-language community for many useful programs.

[1] C. A. Bertulani and P. Danielewicz, *Introduction to Nuclear Reactions* (IOP, Bristol, 2004).
[2] C. J. Joachain, *Quantum Collision Theory*, 3rd ed. (North-Holland, Amsterdam, 1999).
[3] L. Buchmann, R. E. Azuma, C. A. Barnes, J. Humblet, and K. Langanke, Phys. Rev. C **54**, 393 (1996).
[4] R. E. Azuma, L. Buchmann, F. C. Barker, C. A. Barnes, J. M. D'Auria, M. Dombsky, U. Giesen, K. P. Jackson, J. D. King, R. G. Korteling, P. McNeely, J. Powell, G. Roy, J. Vincent, T. R. Wang, S. S. M. Wong, and P. R. Wrean, Phys. Rev. C **50**, 1194 (1994).
[5] J. Refsgaard *et al.*, Phys. Lett. B **752**, 296 (2016)
[6] C. R. Brune, W. H. Geist, R. W. Kavanagh, and K. D. Veal, Phys. Rev. Lett. **83**, 4025 (1999).
[7] A. M. Lane and R. G. Thomas, Rev. Mod. Phys. **30**, 257 (1958).
[8] P. Descouvemont and D. Baye, Rep. Prog. Phys. **73**, 036301 (2010).

[9] P. Tischhauser, R. E. Azuma, L. Buchmann, R. Detwiler, U. Giesen, J. Görres, M. Heil, J. Hinnefeld, F. Kappeler, J. J. Kolata, H. Schatz, A. Shotter, E. Stech, S. Vouzoukas, and M. Wiescher, Phys. Rev. Lett. **88**, 072501 (2002).
[10] P. Tischhauser, A. Couture, R. Detwiler, J. Görres, C. Ugalde, E. Stech, M. Wiescher, M. Heil, F. Käppeler, R. E. Azuma, and L. Buchmann, Phys. Rev. C **79**, 055803 (2009).
[11] J.-M. Sparenberg, Phys. Rev. C **69**, 034601 (2004).
[12] J. Hamilton, I. Overbö, and B. Tromborg, Nucl. Phys. B **60**, 443 (1973).
[13] Z. R. Iwinski, L. Rosenberg, and L. Spruch, Phys. Rev. C **29**, 349 (1984).
[14] J.-M. Sparenberg, P. Capel, and D. Baye, Phys. Rev. C **81**, 011601(R) (2010).
[15] J.-M. Sparenberg, P. Capel, and D. Baye, J. Phys.: Conf. Ser. **312**, 082040 (2011).
[16] C. R. Chen, G. L. Payne, J. L. Friar, and B. F. Gibson, Phys. Rev. C **39**, 1261 (1989).
[17] L. D. Blokhintsev, V. I. Kukulin, A. A. Sakharuk, D. A. Savin, and E. V. Kuznetsova, Phys. Rev. C **48**, 2390 (1993).
[18] A. Pupasov, B. F. Samsonov, J.-M. Sparenberg, and D. Baye, Phys. Rev. Lett. **106**, 152301 (2011).
[19] Yu. V. Orlov, B. F. Irgaziev, and L. I. Nikitina, Phys. Rev. C **93**, 014612 (2016).
[20] J. Humblet, P. Dyer, and B. A. Zimmerman, Nucl. Phys. A **271**, 210 (1976).
[21] J. Humblet, Phys. Rev. C **42**, 1582 (1990).
[22] A. M. Mukhamedzhanov and R. E. Tribble, Phys. Rev. C **59**, 3418 (1999).
[23] C. Brune, Nucl. Phys. A **596**, 122 (1996).
[24] J. Humblet, A. Csótó, and K. Langanke, Nucl. Phys. A **638**, 714 (1998).
[25] P. G. Burke, *R-Matrix Theory of Atomic Collisions* (Springer, Berlin, 2011).
[26] O. L. Ramírez Suárez and J.-M. Sparenberg, Phys. Rev. C **88**, 014601 (2013).
[27] D. Baye and E. Brainis, Phys. Rev. C **61**, 025801 (2000).
[28] D. Baye, M. Hesse, and R. Kamouni, Phys. Rev. C **63**, 014605 (2000).
[29] R. Kamouni and D. Baye, Nucl. Phys. A **791**, 68 (2007).
[30] B. W. Filippone, J. Humblet, and K. Langanke, Phys. Rev. C **40**, 515 (1989).
[31] H. van Haeringen and L. P. Kok, Phys. Rev. A **26**, 1218 (1982).
[32] O. L. Ramírez Suárez, Ph.D. thesis, Université libre de Bruxelles, 2014 (unpublished).
[33] B. F. Irgaziev and Yu. V. Orlov, Phys. Rev. C **91**, 024002 (2015).